

MODELING CHAMBER TRANSPORT FOR HEAVY-ION FUSION

WILLIAM M. SHARP,*† DEBRA A. CALLAHAN, and MAX TABAK
Lawrence Livermore National Laboratory, Livermore, California 94550

SIMON S. YU Lawrence Berkeley National Laboratory, Berkeley, California 94720

PER F. PETERSON University of California Berkeley, Berkeley, California 95720

DALE R. WELCH and DAVID V. ROSE Mission Research Corporation
Albuquerque, New Mexico 87104

C. L. OLSON Sandia National Laboratory, Albuquerque, New Mexico 87107

Received August 13, 2002

Accepted for Publication September 12, 2002

In a typical thick-liquid-wall scenario for heavy-ion fusion (HIF), between 70 and 200 high-current beams enter the target chamber through ports and propagate ~ 3 m to the target. Since molten-salt jets are planned to protect the chamber wall, the beams move through vapor from the jets, and collisions between beam ions and this background gas both strip the ions and ionize the gas molecules. Radiation from the preheated target causes further beam stripping and gas ionization. Because of this stripping, beams for HIF are expected to require substantial neutralization in a target chamber. Much re-

cent research has, therefore, focused on beam neutralization by electron sources that were neglected in earlier simulations, including emission from walls and the target, photoionization by the target radiation, and preneutralization by a plasma generated along the beam path. When these effects are included in simulations with practical beam and chamber parameters, the resulting focal spot is approximately the size required by a distributed radiator target.

KEYWORDS: heavy-ion fusion, chamber transport, simulation

I. INTRODUCTION

Heavy-ion beams for an inertial-fusion driver will likely require some form of neutralization during their final transport to the target. The present generation of indirect-drive targets requires a total particle current exceeding 40 kA divided between perhaps 100 beams, and each beam must have a focal-spot radius on the target of ~ 2 mm. In conceptual chamber designs with thick-liquid inner walls, this final transport distance is typically several meters because it must house neutron shielding, 2 m of molten-salt jets inside the chamber to cushion the detonation, and 1 m additional of standoff so

the jets do not vaporize. Focusing is further complicated by collisions between the beam and vapor from the molten salt, which increase the charge state of beam ions. Although several chamber-transport methods¹ have been proposed for heavy-ion fusion (HIF), the mode currently favored in the U.S. program is “neutralized ballistic” transport. With this method, electrons from collisional ionization or from some external source are entrained by the beam and neutralize the space charge sufficiently that the pulse focuses on the target in a nearly ballistic manner.

In recent years, considerable progress has been made in numerical simulations of neutralized ballistic transport. A useful survey in 1995 by Callahan² indicated that beam stripping due to collisions with the background gas would complicate focusing when thick-liquid walls were used to protect the chamber. Much better focusing

*Current address: William M. Sharp, Lawrence Livermore National Laboratory L-645, Livermore, California 94550.

†E-mail: wsharp@lbl.gov

was found when as little as 0.44% of the background gas was ionized, although uniform ionization even at that low level remains problematic. Both Barboza³ and Vay and Deutsch⁴ reported improvements in numerics for chamber-transport simulations, and some of these advances were incorporated in subsequent work by Sharp et al.⁵ None of this later work, however, changed the original conclusion by Callahan that supplemental neutralization is necessary for successful transport in a chamber protected by thick-liquid walls. In Japan, Kikuchi et al.⁶ have proposed using a dielectric liner in the beam ports to furnish electrons, while the U.S. HIF program is studying the use of injected hydrogen plasma to preneutralize beams.⁷ Recent simulations of foot pulses by Sharp et al.⁸ show that passing a beam through a low-density plasma substantially improves the focal spot, provided that the background-gas density is sufficiently low. In this work, however, the plasma is electrically isolated, reducing its effectiveness. New simulations by Rose et al.⁹ and by Welch et al.¹⁰ show that placing the plasma in contact with conducting walls leads to beam neutralization approaching the theoretical maximum and, consequently, to focal spots of 2 mm or less.

Most of the published work on neutralized chamber transport uses beam and chamber parameters near those chosen by Callahan,² even though conceptual designs of HIF power plants now favor using lighter ions at lower energy and substantially higher current. The simulations in this paper are the first to use beam parameters and a chamber layout derived from recent power-plant studies. These parameters are presented in Sec. II, along with details of the numerical model. In Sec. III, we show that these beams marginally meet the requirements of current target designs. A brief summary and some comments about remaining work are given in Sec. IV.

II. METHOD

II.A. Numerical Model

The axisymmetric chamber-transport simulations reported here were made with the electromagnetic particle-in-cell LSP code,^{11,12} developed by Mission Research Corporation. The code has a relativistic particle advance, allows the use of multiple species, and incorporates models of most physical processes expected in a fusion chamber, particularly electron emission from walls and collisional ionization and scattering. In addition, there are several features that make LSP useful for modeling chamber transport. The problem domain is built from simple geometric forms, allowing the beam port and chamber to be modeled together. The number of macroparticles representing any species can be controlled using an algorithm developed by Lapenta and Brackbill,¹³ so acceptable particle statistics can be maintained despite large differences in the densities of the various species. LSP has an optional implicit integration step, allowing the use of small grid cells when needed without being constrained by a Courant condition. Finally, a rudimentary photoionization model⁵ has been added to LSP for the present work to assess the effects of X rays emitted by the heated target.

The LSP chamber-transport model necessarily includes a wide range of physical processes. A complete representation of the fusion chamber, sketched in Fig. 1, would include neutralization by one or more upstream plasma layers, electron emission from walls, collisional scattering, ionization, and recombination between the beam and background gas, charge buildup on the target, modification of electric fields by the molten-salt jets, and photoionization of the beam, jets, and background

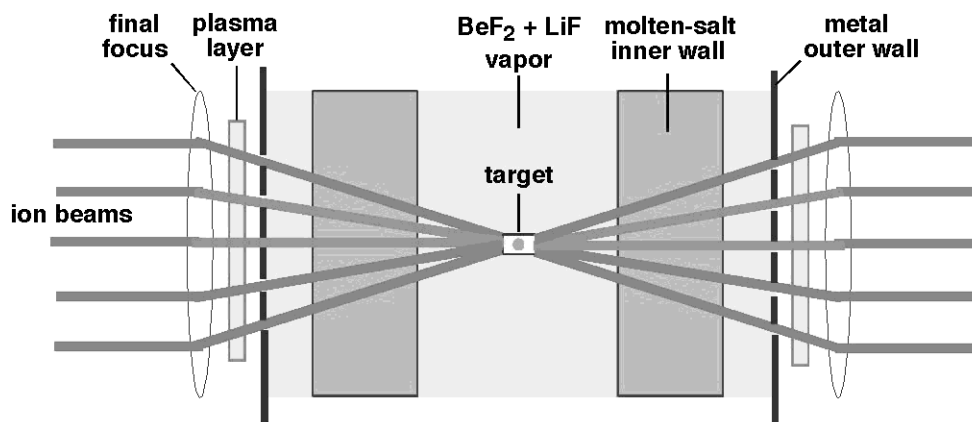


Fig. 1. Sketch of a generic fusion chamber with an indirect-drive target driven on two sides by clusters of ion beams. The thick-liquid walls protecting the chamber, shown as solid shaded areas, would actually consist of crisscrossed jets of molten salt.

gas by X rays from the heated target. The simulations presented here include the most important of these effects, although some, such as collisional scattering and recombination, are estimated to be small and are therefore neglected. Only a single beam is treated, ignoring possible interbeam effects near the target, and the initial beam distribution function is idealized. The beam is assumed to be axisymmetric, with initially uniform density and emittance, and the current is constant except in rise and fall sections near the beam ends. The background gas in the chamber, resulting from the molten-salt jets, is assumed to be initially uniform and neutral, and it falls off with a physically plausible profile in the beam port. Because of the low background-gas density in the chamber, we follow collisional ionization only of neutral gas molecules, although the gas can be ionized to higher charge states by X rays from the target. Background-gas ions are mobile, whereas the hydrogen ions in the neutralizing plasma are not. Runs made with the opposite choices indicate, however, that ion mobility has a negligible effect. Finally, the molten-salt jets themselves are neglected at present, and there is no metal boundary where the target would be, so any problems with target-charge buildup would not appear.

The collisional-ionization cross sections used here were calculated by Olson¹⁴ using a Monte Carlo technique. Electrons liberated by collisions are assigned a Maxwellian energy distribution with an average energy of 20 eV, approximating the distribution calculated by Olson, and their angular distribution is random. In the absence of experimental validation, the Olson cross sections have instead been compared with results from a phenomenological model developed by Armel.¹⁵ This comparison shows good agreement for beam ions with a charge state less than four, and discrepancies seen for higher charge states are not expected to compromise the results significantly, due to the small size of these higher-state cross sections. At present, the LSP model allows only single-electron ionization events, even though calculations¹⁴ suggest that cross sections for multiple-electron ionization are sizeable. Nonetheless, multiple-electron ionization has been studied elsewhere⁸ and is found to have only a minor effect on the neutralization and focal spot of a typical HIF beam.

II.B. Parameters

The simulation parameters used here are based on recent HIF power-plant studies by Meier.¹⁶ The IBEAM design code^{17,18} minimizes the power-plant cost by adjusting parameters in an elaborate set of physics and pricing relationships. This optimization procedure typically involves trade-offs that complicate chamber transport. Lower-energy beams with higher current are favored because the cost of induction accelerators increases in rough proportion with ion energy. However, the lower energy necessitates use of a lower ion mass M to give the same

stopping distance in a target. As discussed in Ref. 8, the current per beam I increases like M^{-1} when the number of beams and their duration are held constant, and the generalized perveance,¹⁹ which is a good measure of space-charge effects, varies like M^{-2} under these conditions. The higher total current needed with lighter ions can be partially mitigated by dividing the current between more beams, but a practical limit is set by achievable packing densities around the chamber, by the maximum angle at which beams can impinge on the target, and by overall system complexity. To increase thermal efficiency, the optimization model also favors a higher temperature for the molten-salt jets, although that choice increases the background-gas pressure and therefore the rate of collisional stripping. Finally, the IBEAM optimization is based on the requirements of distributed-radiator targets.^{20,21} developed at Lawrence Livermore National Laboratory. Unlike previous target designs in which the ends of a cylindrical hohlraum were fully illuminated, this family of targets requires 95% of the beam energy to be deposited in an annulus on each end with a width between 1 and 2.3 mm. Since the space-charge field of a beam scales inversely with the radius, the use of distributed-radiator targets at least doubles the maximum space-charge force of an unneutralized beam and quadruples the peak charge density.

The indirect-drive target described in Ref. 20 requires a total beam energy of 6 to 6.5 MJ. About 1.5 MJ of this total must be delivered in a “foot” pulse, beginning 30 ns before the main pulses arrive, heating the hohlraum to ~ 100 eV and initiating the first shock wave in the capsule. The main pulses then deposit their energy in 8 to 10 ns, launching three more shock waves and igniting the fuel. To compensate for range-shortening as the target is heated, the energy of foot-pulse ions is 75% of the main-pulse ion energy. Following Meier,¹⁶ we use Xe^{+1} ions at 131 amu in the simulations here, with ion energies of 1.9 and 2.5 GeV, respectively, in the foot and main pulses. Foot- and main-pulse currents are taken to be 0.76 and 2.84 kA, respectively, corresponding to a total 112 beams, with 36 foot beams and 76 main beams. The main-pulse current profile has an 8-ns flat top, with 3-ns parabolically varying rise and fall sections at the ends, while the foot-pulse profile has an 18-ns flat top and 6-ns rise and fall sections. Each type of beam has a 6-cm radius as it enters the 3-m beam port, and the beam is focused at a point 3 m inside the chamber wall, giving the beam a 6-m transport distance and an initial convergence angle of 10 mrad. The unnormalized root-mean-square (rms) emittance ε_{\perp} is taken to be initially 9 mm-mrad, but results are not sensitive to this choice, due to the sizable emittance growth during chamber transport.

The chamber simulated here is uniformly filled with a mixture of 90% BeF_2 and 10% LiF , as expected when molten FliBe (Ref. 22) at 600°C is used to protect the chamber wall. Based on experimental work by Olander et al.,²³ the vapor density in the chamber is $7 \times 10^{12} \text{ cm}^{-3}$,

corresponding to ~ 0.2 mTorr. In the 3-m beam port, the density falls off proportionally with $(1 + \Delta z^2/R_2^{port})^{-1}$, where R_{port} is the beam-port radius and Δz is the distance upstream from the chamber. A 10-cm layer of fully ionized hydrogen plasma is placed near each end of the beam port, one centered 36 cm from the entrance and the other, 12 cm from the exit. The electron density in the plasma is 3×10^{11} cm $^{-3}$, although simulation results are not sensitive to this density as long as it exceeds the beam density at the same axial position. The conducting beam-port wall is a cone placed 1 cm outside the nominal beam edge, and electron emission is allowed near the

Q3 plasma layers.

III. RESULTS

III.A. Effects of Preneutralization

To illustrate the effects of the preneutralization alone, we artificially turn off photoionization and compare the dynamics of beams with and without the upstream plasma layers. As found in earlier chamber-transport simulations, the neutralization provided by background-gas ionization for the present parameters is inadequate to allow a usable focal spot. Time histories of the beam rms radius for an unneutralized main pulse, shown in Fig. 2a, indicate that the point of best focus, called the beam “waist,” occurs just as the beam enters the chamber, after 50-ns transport. By the time the beam reaches the nominal target location, ~ 100 ns, the radius is larger than the initial value. When the case is rerun with the addition of plasma layers near the ends of the beam port, $\sim 90\%$ of the beam space charge is neutralized as it enters the chamber, and the minimum radius is ~ 2.6 mm, as seen in Fig. 2b. The waist actually occurs 0.12 m beyond the nominal target location, due to the residual space charge, but this error can be corrected by changing the nominal focal position. Results with foot pulses are

similar, with the radius at the waist location remaining < 2.4 mm when preneutralization is used.

Another series of runs has shown that several factors contribute to the effectiveness of preneutralization. When the same beam is passed through electrically isolated plasmas, the emerging beam is only $\sim 50\%$ charge neutralized since removal of electrons from the plasma builds up a space charge that resists further extraction. Surrounding the beam with a conducting but nonemitting pipe as it passes through the plasma increases the neutralization to nearly 80% because the image charge on the pipe alters the plasma space-charge field and makes it easier to remove electrons along the axis. Finally, permitting electron emission from the conducting wall keeps the plasma quasi-neutral as electrons are extracted, giving $\sim 90\%$ neutralization. This value is close to the theoretical limit for these parameters of $\sim 95\%$, calculated using work by Olson.¹

The effectiveness of preneutralization is found to decrease at higher background-gas densities. At the nominal density of 7×10^{12} cm $^{-3}$, the mean-free-path for background-gas ionization is 4.5 m, which is substantially larger than the 3-m chamber radius. Consequently, neither beam stripping nor background-gas ionization have much effect on beam neutralization. The average charge state of the beam remains less than two, and in the absence of the upstream plasma layers, neutralization from the background climbs to only $\sim 70\%$. In contrast, when the ionization length is short compared with the chamber radius, the neutralization fraction is scarcely different from that of preneutralization alone since that value is already near the theoretical limit, but the beam is stripped to a much higher charge state. As a result, ions feel a larger space-charge force and focus to a larger spot.

III.B. Effects of Beam Convergence Angle

One proposal for reducing the beam focal spot is to increase the initial convergence angle θ_0 . In the absence

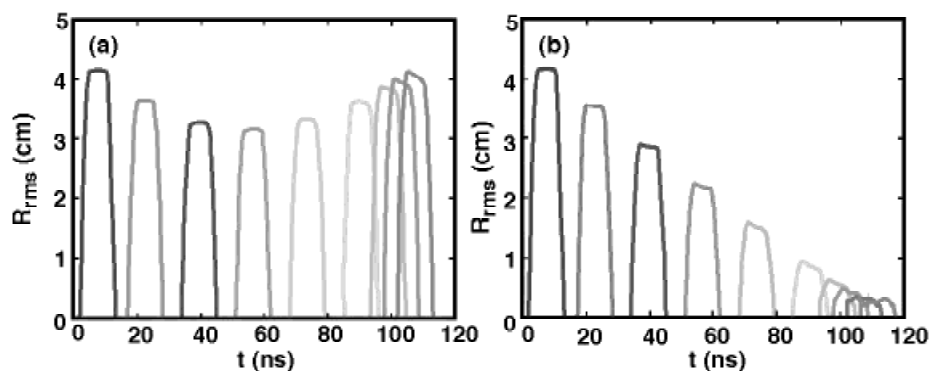


Fig. 2. Time variation of the main-pulse rms radii at selected axial locations (a) with no preneutralization and (b) with preneutralizing plasma placed near the ends of the beam port. Photoionization has been turned off in these simulations.

of space charge, an envelope equation for the beam rms radius predicts a minimum radius of $\varepsilon_{\perp}/\theta_0$ provided that the rms emittance ε_{\perp} is constant. LSP simulations using both the nominal 10-mrad convergence angle and a 15-mrad angle, again with photoionization turned off, show the waist radius varying more weakly with θ_0 than the predicted inverse dependence. The time histories of the main-pulse radius in Fig. 3 show the minimum radius decreasing from 2.6 mm for 10 mrads to 2.2 mm for 15 mrads, which is less than half the predicted 33% decrease. Also, the waist radius for both angles is about a factor of ~ 3 larger than predicted by the envelope model because of the emittance increase during transport. Similar results are found for foot pulses. The maximum radius of a foot pulse decreases from 2.4 mm at 10 mrads to 1.9 mm at 15 mrads, again less than the predicted change. In all these simulations, the analytic expression predicts too small a waist because it ignores emittance growth during transport, which is a factor of ~ 3 for the present parameters. In addition, the expression overestimates the sensitivity to the convergence angle because the beam space charge is imperfectly neutralized, contrary to what was assumed. The unneutralized space charge contributes an additional force that gives a finite waist even for zero emittance.

Although these simulations show some improvement from using a larger convergence angle, there are also several drawbacks. First, the larger beam size in the final-focus magnets would increase the size and cost of that section. Second, the larger entrance holes and gaps between molten-salt jets would allow more neutrons from a fusion target to escape the chamber, complicating the shielding problem. Finally, enlarging each beam line would increase the cone angle of beams approaching the target, forcing the use of a target with lower gain. The cone angle might be held constant by reducing the number of beams, but the current of each beam would then have to be increased appropriately, probably nullifying the improved focal spot. Selecting the optimum conver-

gence angle will require collaboration with target designers and neutronics engineers.

III.C. Effects of Photoionization

Including photoionization by target X rays in the previous case with a 15-mrad convergence angle makes only a modest improvement in chamber transport. Because of the r^{-2} fall-off of the photon density, the effects of photoionization become significant only in the final 50 to 75 cm of transport. One major effect is the increase in the average beam charge state from about 1.8 to more nearly 6, as shown in Fig. 4. This increase, however, has little effect on beam dynamics for two reasons. First, the beam is quite rigid. To bend a 2.5-GeV Xe^{+5} ion by 1 mm over a 50-cm distance requires ~ 8.5 MV/m, a value far exceeding the calculated net field. The second reason for the minor effect on dynamics is that the beam net charge increases relatively little in this region, due to both the abundance of free electrons from background-gas photoionization and to the fact that free electrons from photostripping are nearly comoving with the parent ion. At the beam waist, the net charge inside the beam increases by a factor of ~ 2 when photoionization is turned on, leading to the 20% increase in the rms emittance near the target seen in Fig. 5. This emittance increase, however, is mainly in the transverse velocity and is not reflected in the spot size. In fact, the beam rms radius at the waist location is $\sim 10\%$ smaller than the corresponding case without photoionization, as seen in Fig. 6. This seeming inconsistency occurs because the beam enters the photoionized plasma surrounding the target before it undergoes significant photostripping, so the beam first experiences a period of reduced space charge before the later increase. An examination of the net current for these cases shows that the beam is 80 to 90% current neutralized near the waist, both with and without photoionization. However, because of the higher charge state, the net current is much higher with photoionization, and the

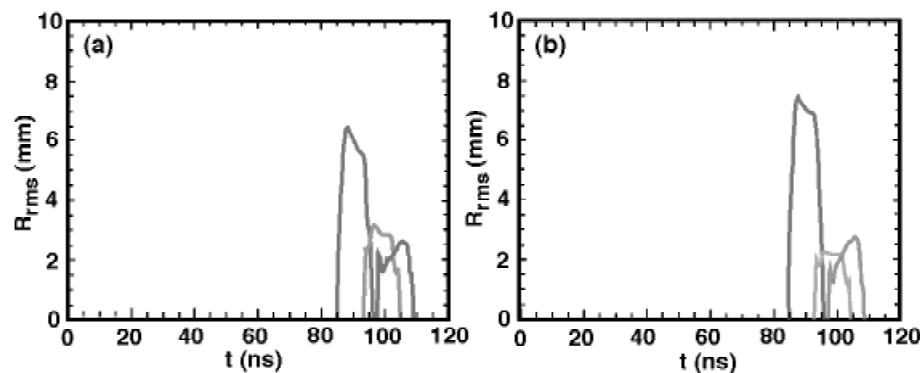


Fig. 3. Time variation of the main-pulse rms radius with (a) a 10-mrad and (b) a 15-mrad initial convergence angle. Photoionization has been turned off in these simulations.

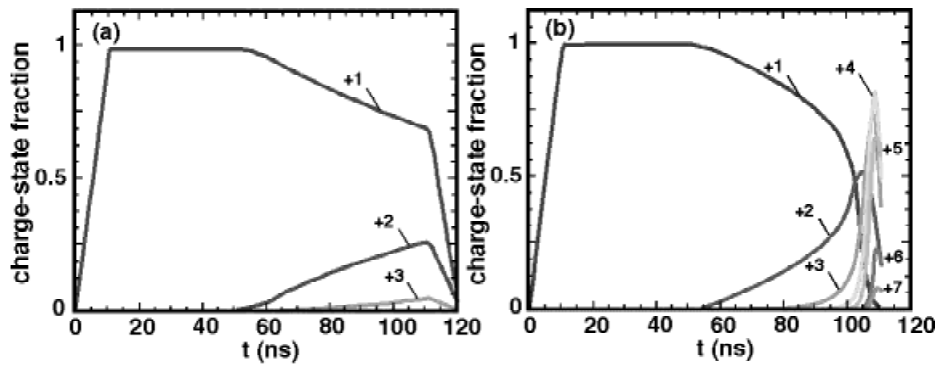


Fig. 4. Time variation of the fraction of main-pulse ions in various charge states (a) without and (b) with photoionization. The beam head reaches the target location after ~ 100 ns.

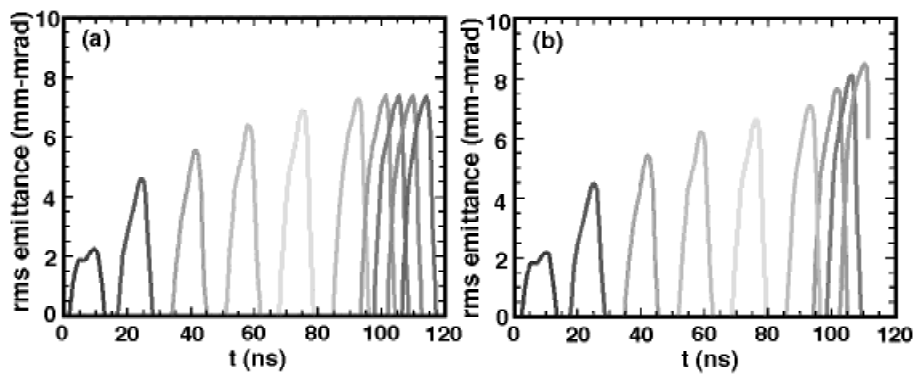


Fig. 5. Time variation of the main-pulse emittance at selected axial positions (a) without and (b) with photoionization.

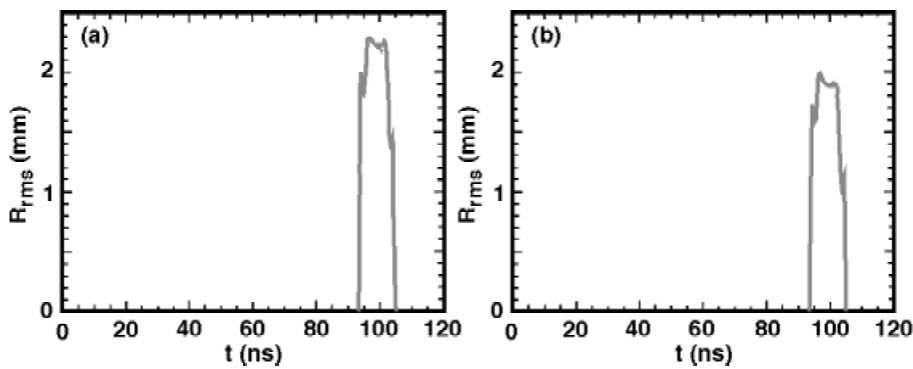


Fig. 6. Time variation of the main-pulse rms radius near the waist (a) without and (b) with photoionization for a 15-mrad convergence angle. An expanded vertical scale is used here to highlight differences.

self-magnetic field approaches 15 kG at its maximum. Nonetheless, the self-magnetic field has a negligible effect on the transverse dynamics for these parameters because it builds up only in the immediate vicinity of the target.

Photoionization has also been included in several foot-pulse simulations. In these cases, photoionization

becomes important only ~ 10 ns after the beam head arrives, due to the time required to heat the hohlraum. The effects of improved charge neutralization are therefore only evident in a 10% reduction in the tail radius of the foot pulse. Since this part of the pulse is needed only for maintaining the hohlraum temperature near 100 eV, this improvement has little importance. However, the

wide-angle distributed-radiator target recently described by Callahan et al.²⁷ requires more than half of the foot-pulse energy to be deposited in the final 8 ns, due to the greater mass near the target midsection. In this case, improved neutralization by a photoionized plasma may significantly improve the transport of this higher-current foot-pulse tail.

IV. CONCLUSIONS

The chamber-transport simulations reported here are the first to use parameters approximating those favored for an HIF driver. The beams have a higher current and lower rigidity than values used in previous simulations, and several previously neglected physical features have been included in the model, such as the 3-m beam ports, multiple ionization of the background gas, and photoionization by target X rays. Both main pulses and the foot pulses used to heat the hohlraum have calculated focal spots that marginally match the requirements of recent distributed-radiator targets. This good performance is largely due to preneutralization by layers of hydrogen plasma near both ends of the beam port. Some improvement in the focal spot results from using a 15-mrad convergence angle instead of the nominal 10-mrad angle, but the larger entrance hole complicates chamber design and neutron shielding. Photoionization further improves the focal spot of main pulses by $\sim 10\%$ but, as expected, has a minimal effect on foot pulses.

Collaboration with target and accelerator designers is still needed to develop an optimized and integrated scenario for chamber transport. In future work, we will determine the most effective choices for the beam convergence angle, and the size and density of the neutralizing plasma. Work is beginning on the use of more realistic input beam distributions, including the time variation of the foot-pulse current, and several additional features of chamber physics will be added to the numerical model, particularly some representation of the molten-salt jets.

ACKNOWLEDGMENTS

This work was performed under the auspices of the U.S. Department of Energy by University of California Lawrence Livermore National Laboratory and Lawrence Berkeley National Laboratory under Contracts W-7405-ENG-48 and DE-AC-3-76SF00098.

REFERENCES

1. C. L. OLSON, *Nucl. Instrum. Methods Phys. Res. A*, **464**, 118 (2001).

2. D. A. CALLAHAN, *Fusion Eng. Des.*, **32–33**, 441 (1995).
3. N. BARBOZA, *Fusion Eng. Des.*, **32–33**, 453 (1995).
4. J.-L. VAY and C. DEUTSCH, *Fusion Eng. Des.*, **32–33**, 467 (1995).
5. W. M. SHARP, D. A. CALLAHAN-MILLER, A. B. LANGDON, M. S. ARMEL, and J.-L. VAY, *Nucl. Instrum. Methods Phys. Res. A*, **464**, 284 (2001).
6. T. KIKUCHI, S. KAWATA, S. KATO, S. HANAMORI, and M. YAZAWA, *Jpn. J. Appl. Phys.*, **3**, 270 (1999).
7. P. C. EFTHIMION and R. C. DAVIDSON, *Nucl. Instrum. Methods Phys. Res. A*, **464**, 310 (2001).
8. W. M. SHARP, D. A. CALLAHAN-MILLER, M. TABAK, S. S. YU, and P. F. PETERSON, "Chamber Transport of 'Foot' Pulses for Heavy-Ion Fusion," *Phys. Plasmas* (submitted for publication).
9. D. V. ROSE, D. R. WELCH, B. V. OLIVER, W. M. SHARP, and A. FRIEDMAN, *Nucl. Instrum. Methods Phys. Res. A*, **464**, 299 (2001).
10. D. R. WELCH, D. V. ROSE, B. V. OLIVER, T. C. GENONI, and R. E. CLARK, *Phys. Plasmas*, **9**, 2344 (2002).
11. T. P. HUGHES, R. E. CLARK, and S. S. YU, *Phys. Rev ST Accel. Beams*, **2**, 110401 (1999). Q1
12. D. R. WELCH, D. V. ROSE, B. V. OLIVER, and R. E. CLARK, *Nucl. Instrum. Methods Phys. Res. A*, **464**, 134 (2001).
13. G. LAPENTA and J. U. BRACKBILL, *J. Comput. Phys.*, **115**, 213 (1994).
14. R. E. OLSON, *Nucl. Instrum. Methods Phys. Res. A*, **464**, 93 (2001).
15. M. S. ARMEL, "Atomic Processes for Heavy Ion Inertial Fusion," PhD Thesis, University of California, Berkeley (2000).
16. W. R. MEIER, Private Communication.
17. W. R. MEIER, R. O. BANGERTER, and A. FALTENS, *Nucl. Instrum. Methods Phys. Res. A*, **415**, 249 (1998).
18. W. R. MEIER, J. J. BARNARD, and R. O. BANGERTER, *Nucl. Instrum. Methods Phys. Res. A*, **464**, 433 (2001).
19. J. D. LAWSON, *J. Electron. Control*, **5**, 146 (1958).
20. M. TABAK and D. A. CALLAHAN-MILLER, *Nucl. Instrum. Methods Phys. Res. A*, **415**, 75 (1998).
21. D. A. CALLAHAN-MILLER and M. TABAK, *Nucl. Fusion*, **39**, 1547 (1999).
22. R. W. MOIR et al., *Fusion Technol.*, **25**, 5 (1994).
23. D. R. OLANDER, G. FUKUDA, and C. F. BAES, Jr., *Fusion Sci. Technol.*, **41**, 141 (2002).

Sharp et al. HIF CHAMBER TRANSPORT

24. M. REISER, *Theory and Design of Charged Particle Beams*, p. 341ff., John Wiley & Sons, New York (1994).
25. A. B. LANGDON, R. O. BANGERTER, and D. A. LIBERMAN, *Nucl. Instrum. Methods Phys. Res. A*, **278**, 68 (1989).
26. A. B. LANGDON, *Part. Accel.*, **37-38**, 175 (1992).
27. D. A. CALLAHAN-MILLER, M. C. HERRMANN, and M. TABAK, "Progress in Heavy Ion Target Capsule and Hohlraum Design," *Laser Part. Beams*, **20**, 405 (2002).

William M. Sharp (BS, Harvey Mudd College, 1968; MS, 1969, and PhD, 1976, applied science, University of California, Davis) works as a physicist at Lawrence Livermore National Laboratory (LLNL) and is responsible for modeling the transport of ion beams through an inertial-fusion chamber.

Debra A. Callahan (BS, physics and mathematics, University of Denver, 1985, MS, 1989, and PhD, 1994, applied science, University of California, Davis) is a physicist at LLNL and is responsible for designing targets for heavy-ion-driven, inertial-fusion energy. Her research interests are inertial-confinement fusion and fusion energy.

Max Tabak (BS, physics, Massachusetts Institute of Technology, 1970; PhD, physics, University of California, 1975) is a group leader in the AX Division at LLNL, as well as the associate program leader for inertia fusion energy target design in the Fusion Energy Program at LLNL. His current research interests include fast ignition and heavy-ion target design.

Simon S. Yu (BS, physics, Seattle Pacific University, 1963; MS and PhD, physics, University of Washington, 1970) is a senior staff scientist at the Lawrence Berkeley National Laboratory. He is the leader of the Heavy-Ion Final-Focus Group.

Per F. Peterson (BS, mechanical engineering, University of Nevada, Reno, 1982; MS, 1986, and PhD, 1988, mechanical engineering, University of California, Berkeley) is professor and chair of the Department of Nuclear Engineering at the University of California, Berkeley. His research interests focus on topics in heat and mass transfer, fluid dynamics, and phase change, with applications to inertial fusion energy, advanced reactors, and nuclear materials management.

Dale R. Welch (BS, nuclear engineering, Northwestern University, 1980; MS, 1982, and PhD, 1985, nuclear engineering, University of Illinois) works for Mission Research Corporation, where he is involved with the investigation of beam transport and plasma modeling in pulsed-power machines.

David V. Rose (BA, physics, Temple University, 1986; MS, applied physics, Johns Hopkins University, 1991; PhD, computational physics, George Mason University, 1997) is a senior research physicist with Mission Research Corporation, in the Particle Beam and Hydrodynamic Group. His research interests include fundamental plasma physics, high-energy astrophysics, and fusion energy.

Q2